

Training-Free Exponential Extension of Sliding Window Context with Cascading KV Cache

Jeffrey Willette¹ Heejun Lee¹ Youngwan Lee^{1,3} Myeongjae Jeon² Sung Ju Hwang^{1,4}
 KAIST¹ UNIST² ETRI³ DeepAuto.ai⁴
 {jwillette, sjhwang82}@kaist.ac.kr

Abstract

The context window within a transformer provides a form of active memory for the current task, which can be useful for few-shot learning and conditional generation, both of which depend heavily on previous context tokens. However, as the context length grows, the computational cost increases quadratically. Recent works have shown that saving a few initial tokens along with a fixed-sized sliding window leads to stable streaming generation with linear complexity in transformer-based Large Language Models (LLMs). However, they make suboptimal use of the fixed window by naively evicting all tokens unconditionally from the key-value (KV) cache once they reach the end of the window, resulting in tokens being forgotten and no longer able to affect subsequent predictions. To overcome this limitation, we propose a novel mechanism for storing longer sliding window contexts with the same total cache size by keeping separate cascading sub-cache buffers whereby each subsequent buffer conditionally accepts a fraction of the relatively more important tokens evicted from the previous buffer. Our method results in a dynamic KV cache that can store tokens from the more distant past than a fixed, static sliding window approach. Our experiments show improvements of 5.6% on long context generation (LongBench), 1.2% in streaming perplexity (PG19), and 0.6% in language understanding (MMLU STEM) using LLMs given the same fixed cache size. Additionally, we provide an efficient implementation that improves the KV cache latency from 1.33ms per caching operation to 0.54ms, a 59% speedup over previous work.

1 Introduction

A key problem in deploying large language models (LLMs) is the compute cost necessary to perform the attention [20] operation during inference. While there have been key advancements such as FlashAttention [6], which lower the memory burden by never creating the full attention matrix in memory, the latency and compute costs still grow quadratically with input size. This poses a problem for streaming very long input sequences, as there will be a significant latency in generation, incurring high costs and impairing user experiences.

While there are existing methods for handling long sequences with sliding windows [3, 9], the window size presents a static barrier to long-term context memory, as it will eventually start naively evicting tokens, which will be forgotten from the context history forever. Recent works have proposed keeping a small number of tokens from the beginning of the sequence in addition to a standard sliding window

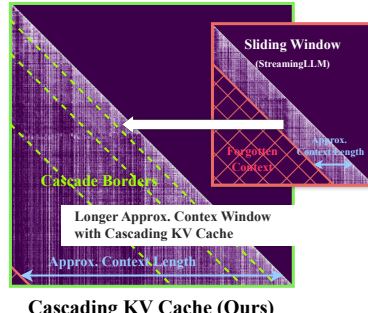


Figure 1: Attention matrices from Streaming LLM [21] and Cascading KV Cache (Ours), **both with the same total cache size**.

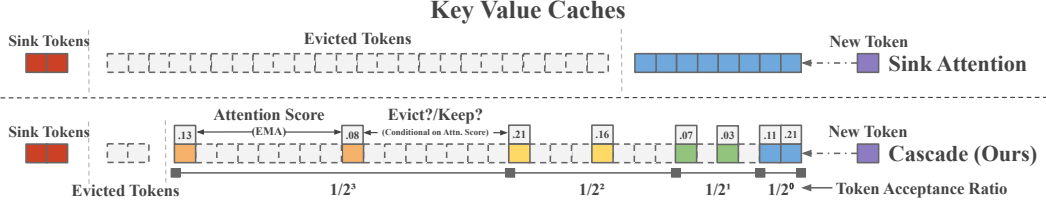


Figure 2: Comparison of Streaming LLM (Sink Cache) [21] and Cascading Cache (Ours). **Top:** Sink Cache stores **fixed sink tokens (red)** along with a **sliding window** of N recent tokens. **Bottom:** Our method segments the cache into smaller cascading sub-caches, where each successive sub-cache conditionally accepts a fraction of tokens based on the magnitude of past attention scores. This simple technique allows for important tokens from the distant past to remain in the cache for a longer period of time instead of being naively evicted and forgotten forever.

KV cache as a way to stabilize the sliding window during inference [21] (Figure 2 top). However, the sliding window KV cache is still a static fixture that starts evicting tokens based solely on their position within the sequence and without regard to their overall importance within the context. Other lines of work aim to compress older contexts into a fixed size with a subsequent retrieval mechanism to decompress or retrieve the contexts [14, 13]. However, these methods require further training of a new mechanism to be deployed in conjunction with the underlying transformer.

We aim to overcome the following challenges: **1)** Extend the context memory limitations of sliding window attention with a KV cache while providing a linear complexity at test time. **2)** Provide a training-free method which can be deployed on top of legacy pre-trained quadratic transformers. We provide a solution to these challenges by proposing a simple and effective method for extending the available historical context within sliding window KV caches. Our method views the cache as a collection of sub-caches, each accepting tokens with a different frequency. Additionally, our method utilizes a conditional eviction policy that selectively evicts tokens with lower historical attention scores which are tracked by a layerwise exponential moving average (EMA). This allows for retaining older, but relatively more important tokens in the cache for a longer period of time.

To demonstrate the limitations of a static window and the benefit of our method, we provide two motivating examples: **1)** Figure 1 shows an attention matrix from the PG19 [16] test set. Streaming LLM [21] uses a static window and loses all tokens from the red region once they exit the cache’s sliding window. Our Cascading KV cache populates the majority of the attention matrix using the **same cache size** of the fixed window. **2)** Figure 3 shows a toy example on the Wikitext [12] test set. We compare our method to the static window (both of size 1024) of sink cache [21]. After a burn-in period to populate the key-value caches, we go back a total distance of 2048 tokens (double the distance of the naive sliding window) and restart the stream for 1024 tokens. In this setting, we are restarting the stream so that the model sees 1024 tokens which have already been seen but will have been evicted from the static window. Our method consistently outperforms static window attention for all models and sizes, with a 33.1% lower average perplexity due to the longer effective context length. Our contributions in this work are as follows:

- We propose a simple yet effective modification to sliding window attention, which allows for selectively retaining important past tokens instead of naively discarding tokens when they reach the end of the cache window.
- Our method can be applied on top of any existing pretrained transformers with zero training for linear complexity streaming inference.
- Given the same total KV cache size, our method delivers an improvement of 5.6% in long context benchmarks (LongBench), 1.2% in streaming perplexity (PG19), and 0.6% in Multitask Language Understanding (MMLU).
- We provide an efficient implementation of our KV cache utilizing the Triton Compiler [18] and circular buffers, which achieves a 59% speedup over [21].

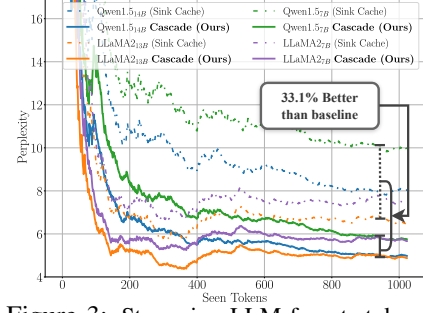


Figure 3: Streaming LLM forgets tokens evicted from the cache (dotted lines). **Ours** (solid lines) keeps some of these tokens, achieving lower ppl. for the same cache size.

2 Related Work

Our work directly builds on ideas which were proposed by Streaming LLM (Sink Cache) [21], which found that many layers of a transformer tend to stop focusing on much of the input sequence and ‘offload’ the attention scores onto the first few tokens in the sequence (the sink tokens). The peculiar pattern has profound consequences when attempting to add a traditional fixed sliding window onto a pretrained quadratic model, as the sink tokens may have already been evicted from the window and the attention is forced to redistribute the same attention score mass onto the tokens that are in the window. Xiao et al. [21] showed that this redistribution of attention scores causes naive sliding window attention to severely degrade in performance unless the first tokens are maintained as part of the sequence. Our work builds on this prior breakthrough and provides a way to extend the context length of the sliding window, given the same total cache size.

Enforcing sparsifying patterns into attention matrices has been shown to be effective in previous works [3], however such patterns may be both heuristic and require training of the underlying model, which can be prohibitively expensive. Linear attention methods have been proposed by way of locality-sensitive hashing [11], kernel approximations [5], or by adding extra token compressive modules [14, 10]. However, each of these requires training either from scratch or on top of existing pretrained models. Our method, however, delivers a training-free inference adaptation to achieve linear attention with dynamic sparsity in the attention matrix.

3 Method

Notation. We use the common notation of a boldface lowercase letter to denote a vector \mathbf{x} and a boldface uppercase letter to denote a matrix \mathbf{X} . \mathbb{N} and \mathbb{R} refer to sets of the natural and real numbers, respectively. A superscript (l) denotes that the object belongs to layer l , where $l \in [1, 2, \dots, L]$. To simplify notation for attention, we omit the head dimension, output projections, and multi-layer perceptron (MLP) transformations, please see Vaswani et al. [20] for an overview regarding those topics. We refer to a generic cache as \mathbf{C} , using subscripts \mathbf{C}_K and \mathbf{C}_V to refer to key and value caches, respectively.

Attention. Let $S \in \mathbb{N}$ represent a token sequence length, where each token at layer l is represented by a vector $\mathbf{x}_i^{(l)} \in \mathbb{R}^d$. The collection of tokens in the sequence can be represented as a matrix $\mathbf{X}^{(l)} \in \mathbb{R}^{S \times d}$. With σ being the softmax function, and different learnable query, key, and value matrices $\mathbf{Q}^{(l)}, \mathbf{K}^{(l)}, \mathbf{V}^{(l)} \in \mathbb{R}^{d \times d}$ the standard attention operation is as follows:

$$\mathbf{X}^{(l+1)} = \sigma \left(\frac{1}{\sqrt{d}} \left(\mathbf{X}^{(l)} \mathbf{Q}^{(l)} \right) \left(\mathbf{X}^{(l)} \mathbf{K}^{(l)} \right)^\top \right) \mathbf{X}^{(l)} \mathbf{V}^{(l)} \in \mathbb{R}^{S \times d} \quad (1)$$

Key-Value (KV) Caching. During LLM inference, a single token is generated at each time step. Combined with a causal attention mask such that token \mathbf{x}_i cannot influence \mathbf{x}_j iff $i > j$, it becomes more efficient to cache the $\mathbf{K}^{(l)}$ and $\mathbf{V}^{(l)}$ projected tokens in each layer l rather than recomputing the full set of key, and value projections at each generation time step. Specifically, for the key and value caches \mathbf{C}_K and \mathbf{C}_V , and with \cup representing a concatenation operation along the S dimension, the calculation of the attention operation for the current token \mathbf{x}_j during inference becomes,

$$\mathbf{x}_j^{(l+1)} = \sigma \left(\frac{1}{\sqrt{d}} \left(\mathbf{x}_j^{(l)} \mathbf{Q}^{(l)} \right) \left(\mathbf{C}_K^{(l)} \cup \left(\mathbf{x}_j^{(l)} \mathbf{K}^{(l)} \right) \right)^\top \right) \left(\mathbf{C}_V^{(l)} \cup \left(\mathbf{x}_j^{(l)} \mathbf{V}^{(l)} \right) \right) \in \mathbb{R}^d \quad (2)$$

After the concatenation operation, $\mathbf{x}_j^{(l)} \mathbf{K}^{(l)}$ and $\mathbf{x}_j^{(l)} \mathbf{V}^{(l)}$ are considered to be added to the \mathbf{C}_K and \mathbf{C}_V caches for the next iteration in the sequence.

Sliding window attention, as used by Beltagy et al. [3], Xiao et al. [21], treats the KV cache as a fixed size buffer which must delete tokens from the cache when the cache reaches its storage limit. Considering a cache which is fully populated (denoted by an overbar $\overline{\mathbf{C}}_K^{(t)}$ and omitting the layer index l), when a new token comes in, the cache must drop the oldest token in order to make space for the new token such that,

$$\overline{\mathbf{C}}_K^{(t+1)} = \overline{\mathbf{C}}_K^{(t)} \cup \mathbf{x}_j \mathbf{K} = [\{\mathbf{x}_i \mathbf{K}, \dots, \mathbf{x}_{j-1} \mathbf{K}\} \cup \{\mathbf{x}_j \mathbf{K}\}] \setminus \{\mathbf{x}_i \mathbf{K}\}. \quad (3)$$

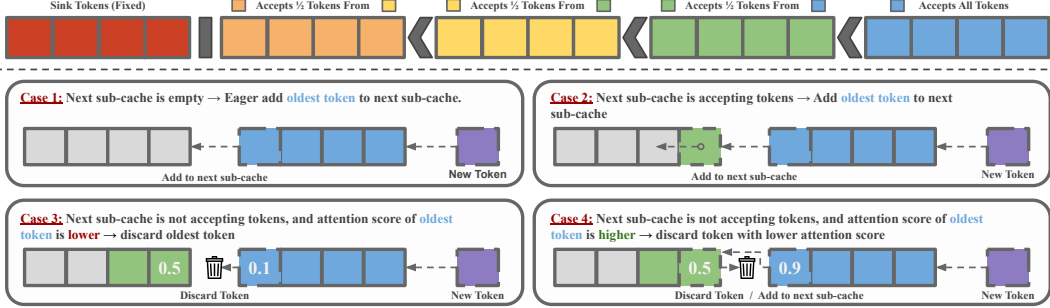


Figure 4: **Top:** Each successive sub-cache window accepts a fraction of tokens evicted from the previous sub-cache. **Bottom:** At the boundaries between sub-caches, there are four possible cases where our method takes a different conditional action, creating a dynamic attention pattern.

The only difference between standard sliding window attention and the sink cache of Streaming LLM [21] is that sink cache perpetually retains the first α tokens in the sequence such that if the cache starts from $i = 1$, it is not token $x_1 \mathbf{K}$ which is evicted, but token $x_{1+\alpha} \mathbf{K}$, with $\alpha \in \mathbb{N}$ being a fixed hyperparameter. Both sliding window attention and sink cache have the benefit of linear complexity, and a fixed overhead computation and memory cost for the window, as the size of the cache can only grow to a fixed, predetermined amount. However, this has the downside of constraining the information available in the cache, which may be needed for later predictions in the sequence. To illustrate, imagine streaming generation of an entire book with an LLM. If the cache can only contain tokens representing the average length of one chapter, then important information from previous chapters may be forgotten which could prove to be crucial for continuity in generation.

3.1 Cascading Cache

We propose a simple modification to sliding window attention via a KV cache that allows older tokens to be kept in the cache history for a longer period of time. To accomplish this, we view a fixed sized sliding window KV cache C with cardinality $|C|$ as a collection of sub-caches C_i for $i \in [1, \dots, N]$, each with cardinality $|C_i| \leq |C|$ such that $|\bigcup_{i=1}^N C_i| = |C|$. Assuming a sub-cache is full, each full sub-cache C_i evicts tokens when a new token is accepted into the sub-cache. However, each sub-cache accepts new tokens at a different rate, which in turn means that tokens may be discarded between the sub-caches and not solely at the end of the total cache window. An example of this process is depicted in Figure 4 (top), where the blue cache accepts all new incoming tokens. The green sub-cache, however, accepts only half of the tokens which are evicted from the blue sub-cache (every 2nd iteration). The yellow sub-cache accepts half of the tokens evicted from the green sub-cache (every 4th iteration) and so on.

As Xiao et al. [21] discovered, the initial attention sink tokens are crucial for the stability of the streaming process, so we too keep a fixed sub-cache of the earliest tokens as attention sinks. The rate at which each cache accepts new tokens may be modified at will by setting a different function which decides the policy as a hyperparameter. Note that with our method, a sink cache is a special case of a cascading cache, where the number of cascades (sub-caches) is set to 1, and it accepts all incoming tokens (*i.e.* using only the blue cache *and* red cache in Figure 4).

Approximate Context Length. We define the approximate context length to be measured based on the total span of the original token indices which currently reside in the cache. The process outlined above effectively extends sliding window context length by allowing older tokens to remain as keys and values for a longer time, albeit with larger and larger gaps between tokens. Assuming that each sub-cache has the same capacity (*i.e.* $|C| = |\bigcup_i^N C_i| = N|C_1|$), and each will accept tokens with a different frequency function defined as $\frac{1}{f(i)}$, then the approximate context length will be a summation over the cache sizes and the inverse of the frequency functions. For example, if each successive sub-cache accepts half of the tokens evicted from the previous cache, the approximate context length \tilde{L} becomes,

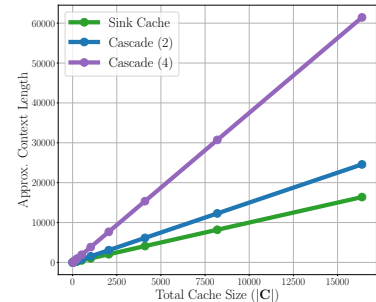


Figure 5: Approximate context length as a function of total window size. $|C| = 4096$

$$\tilde{L} = \sum_{i=1}^N f(i)|C_i| = |C_1| \sum_{i=1}^N 2^{i-1} = \frac{|C|}{N} \sum_{i=1}^N 2^{i-1}. \quad (4)$$

Equation (4) shows the same setting depicted in Figure 4, for example the yellow sub-cache will unconditionally accept new tokens on every 4th iteration. The scaling of the effective context length is shown in Figure 5. Given the same total cache size overhead, our method is able to maintain an increased approximate context length. We ensure that the older stored tokens are important by the token selection process described next. We note, however, that there is a tradeoff when adding more sub-caches, as $|C_1| = |C|/N$, and therefore the number of sub-caches and the overall sparsity grows with an increasing N .

Token Selection. The process outlined in the preceding paragraph would result in a fixed heuristic pattern of tokens being dropped. However, such a heuristic pattern is not ideal, as it may be the case that the model naively holds onto tokens with limited value, while discarding important tokens. To remedy this, instead of discarding tokens naively, we dynamically select the most important tokens to retain by tracking the average attention score each token receives throughout time via an EMA. We then selectively discard the token with the lower attention score EMA where possible. Given a hyperparameter $\gamma \in [0, 1]$, and a vector of attention scores for all keys in the cache $s_k^{(t)}$ at timestep t , we update the stored average attention scores $\mu^{(t)}$ as, $\mu^{(t+1)} = \gamma \mu^{(t)} + (1 - \gamma) s_k^{(t)}$.

Consider the two sub-caches depicted in cases 2-4 of Figure 4. The blue sub-cache must accept all incoming tokens, while the green cache only accepts tokens every other iteration. Let the green cache be accepting tokens at the current timestep (case 2). A new token comes in and is added to the blue cache which must then evict a token since it is full. The evicted token then goes to the green cache which accepts it unconditionally. The same process repeats on the next iteration, however, this time the green cache will not be accepting tokens (cases 3-4). At this step, when the blue cache accepts and evicts a token, we compare the attention score of the token evicted from the blue cache with the attention score of the rightmost token in the green cache. The token with the higher attention score is set (or remains) as the rightmost token in the green cache, while the token with the lower attention score is discarded. For a full pseudocode algorithm the covers cases 1-4 in Figure 4, please see Algorithm 1 in the appendix.

During this token selection process, we ensure that we perform the same retention/eviction action over all attention heads in order to maintain a single positional encoding for each token in the cache (for more detail on why this is necessary, please see Appendix C). Therefore, before updating the token attention score EMA, we perform a reduction of the scores over the attention heads, which can be any sum decomposable reduction function $\rho : \mathbb{R}^d \mapsto \mathbb{R}$, such as $\{\max, \text{median}, \text{mean}\}$.

Positional Encoding. We use the same positional encoding strategy as Xiao et al. [21], which keeps the positional encodings for each token relative and applies positional encodings consecutively, starting with the 0 index. With $\text{PE}_{\text{index}} : \mathbb{N} \mapsto \mathbb{N}$ signifying a positional encoding index function, and $i, j \in \mathbb{N}$ representing the original token positions in the input sequence, it follows that $i < j \iff \text{PE}_{\text{index}}(i) < \text{PE}_{\text{index}}(j)$. For example, if our cascading cache holds the token indices from the original sequence $[0, 1, 3, 5, 7, 8]$, they would in turn receive positional encodings $[0, 1, 2, 3, 4, 5]$.

4 Experiments

Setup. We conduct experiments on a subset of the PG19 test set [16], LongBench [2], and the massive multitask language understanding dataset (MMLU) [8] STEM subset. We evaluate our method using the pretrained transformers Llama2 7B/13B [19] and Qwen1.5 7B/14B [1]. Please see Table 11 for pretrained model paths. In all our experiments, we keep the first 4 initial tokens as attention sinks, as this was a common setting in Xiao et al. [21]. When considering the number of tokens in the cache, we always consider the sink tokens to be in addition to the window size. Therefore a window size of 1024 has a total of 1028 tokens when accounting for the 4 initial sink tokens. We set the head reduction function for token selection to ‘mean’ as a sensible default. We set the EMA parameter to $\gamma = \exp(-N \ln(100)/|C|)$ which depends on the cascade window size. See Appendix B for a derivation. We use the cascade token acceptance setting depicted in Figure 4 and Equation (4), where each sub-cache accepts half of the tokens from the previous sub-cache.

Table 1: Our Cascading KV cache outperforms the fixed window of Sink Cache [21] on PG19 due to maintaining a longer context history. HyperAttention and Full Attention (quadratic) are limited by the number of positional encodings, so they are evaluated on a 32k max sequence length and values are repeated for rows containing different window sizes. Lower scores are better

Window Size	Model	Methods (\downarrow)					
		Vanilla	HyperAttention (All Lyrs.)	HyperAttention (3/4 Lyrs.)	Sink Cache	Cascade (Ours)	
2048	Qwen1.5 _{7B}	9.11 (0.00)	16.27 (+7.16)	19.58 (+10.47)	9.70 (+0.59)	9.52 (+0.41)	
	Qwen1.5 _{14B}	8.50 (0.00)	10.63 (+2.13)	10.50 (+2.00)	9.07 (+0.57)	8.87 (+0.37)	
	LLaMA2 _{7B}	6.67 (0.00)	980.08 (+973.41)	223.35 (+216.68)	7.05 (+0.38)	6.97 (+0.30)	
	LLaMA2 _{13B}	6.18 (0.00)	349.35 (+343.17)	22.26 (+16.08)	6.32 (+0.14)	6.29 (+0.11)	
4096	Qwen1.5 _{7B}	9.11 (0.00)	16.27 (+7.16)	19.58 (+10.47)	9.44 (+0.33)	9.33 (+0.22)	
	Qwen1.5 _{14B}	8.50 (0.00)	10.63 (+2.13)	10.50 (+2.00)	8.82 (+0.32)	8.69 (+0.19)	
	LLaMA2 _{7B}	6.67 (0.00)	980.08 (+973.41)	223.35 (+216.68)	6.90 (+0.23)	6.84 (+0.17)	
	LLaMA2 _{13B}	6.18 (0.00)	349.35 (+343.17)	22.26 (+16.08)	6.19 (+0.01)	6.18 (0.00)	

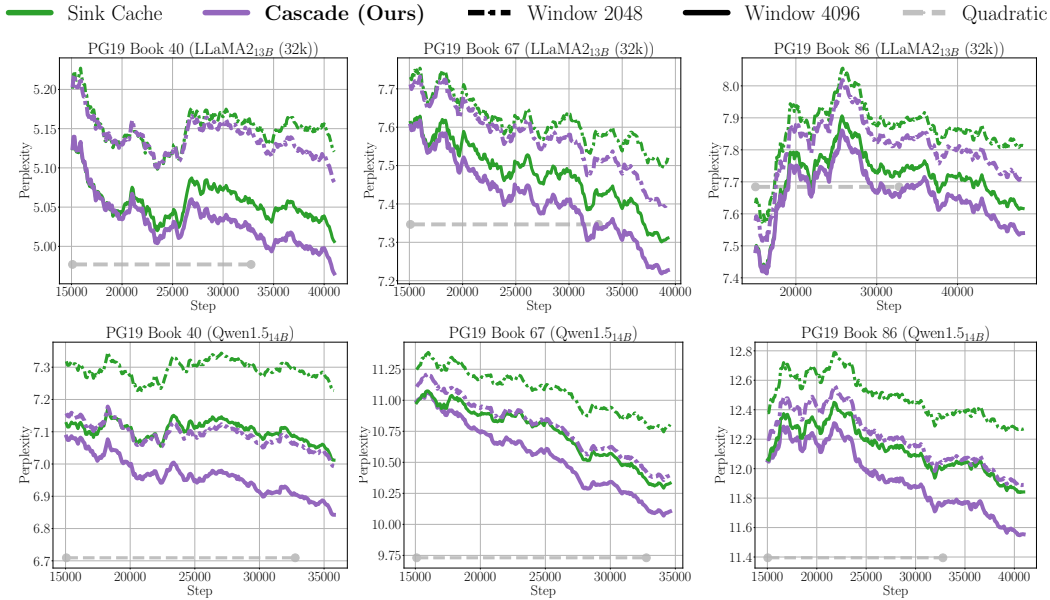


Figure 6: PG19 Streaming results for LLaMA2_{13B} and Qwen1.5_{14B}. The line on each chart represents the average perplexity over the entire sequence. The initial portion of the stream is truncated for better visualization.

4.1 PG19

We measure overall perplexity on a subset of the PG19 [16] test set consisting of 25 full-length books. Each book is streamed independently from start to finish without concatenation. We compare against the vanilla quadratic model as well as hyper attention [7], and sink cache [21] which are also training-free inference adaptations. We use 4 cascading sub-caches ($N = 4$) for our models which gives an approximate context length of 7680 and 15360 for total window sizes $|C|$ of 2048 and 4096, respectively. Tabular results are displayed in Table 1. Our method delivers a consistently lower perplexity for all tested cache and model sizes. Additionally, we show the trend throughout the entire stream of individual books (Figure 6), where each step in the plotted line represents the average perplexity of the entire stream up until the current step. Additional plots for all books can be seen in the appendix in Figures 11 to 14. We show the latter portion of the stream for better visualization. Throughout the stream, our model shows a tendency to have a slowly widening gap in performance between sink cache. Averaged over all scores, our method provides a 1.2% relative lower perplexity than sink cache. Intuitively, our longer context history aids in streaming perplexity, as the cache is able to retain more distant information within the book. For further details regarding the PG19 experiment, please see Appendix D.

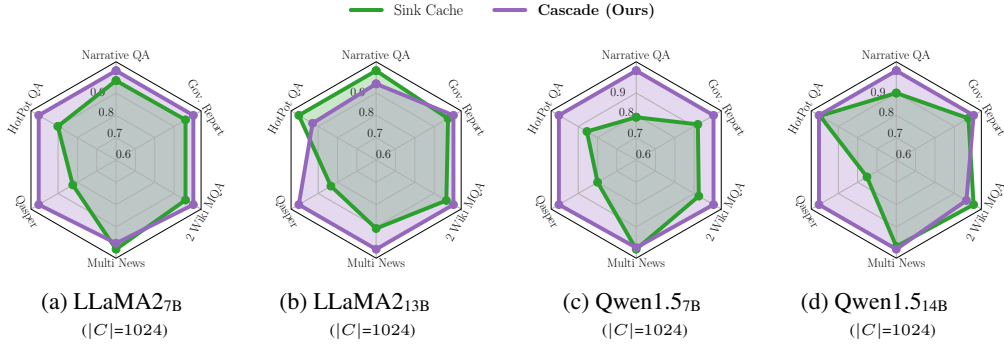


Figure 7: LongBench [2] results, our method shows an increased coverage area over all datasets. For visualization, each slice of the radial plots is normalized by the max of the values within the slice (*i.e.* $x / \max(x)$). For tables and additional results, please see Table 8 and Figure 9.

4.2 LongBench

We evaluate our method on the same subset of tasks as [21] in the LongBench long context benchmark [2]. We use 4 cascading sub-caches ($N = 4$) which deliver an approximate context length of 3840 and 7680 for total cache sizes $|C|$ of 1024 and 2048, respectively. The results are displayed in Figure 7, and in Table 8 and Figure 9 in the appendix. Averaged over all benchmarks and for all models tested, our cascading cache improves performance over sink cache by 5.6%. We found the Qwen model to outperform Llama by a large margin in this task regardless of the caching method. Averaging all Llama and Qwen scores from Table 8 we can see that Llama only achieved 55% of the performance of Qwen on average. This is the opposite of the trend which was observed in the PG19 experiment (Table 1), where Llama excelled. When comparing the differences between our method and the baseline on each base model, we find that our method improved the stronger model (Qwen) by 7.3% over the sink cache baseline, while we improved the performance of the weaker model (Llama) by 2.6%.

4.3 MMLU

We compare our model on the STEM subjects of the MMLU [8] benchmark against sink cache. This task consists of multiple-choice questions, each with 4 possible answers expressed as single letters. Each model receives the same 20 example questions (with answers) from the training set before being asked a target question from the test set. This forms a 4-way/20-shot, few-shot learning problem. The average context length within the STEM subset averages 2100. For this task, both models utilize a window size of 1024 with 4 extra sink tokens. For cascading cache, we use 2 cascading sub-caches ($N = 2$), which brings the approximate context length to 1536. This is not much longer than the 1024 which the baseline sink cache model received, and yet our model still managed to have an overall edge (0.6% improvement) over sink cache in Table 2. For individual subject results, please see Figures 17 and 18.

4.4 Ablation Study

To study each component of our method, we perform an ablation study on the cascade function (Table 5, top-left), head reduction (Table 5, top-right), number of cascades (Table 5, bottom), and token selection (Table 3) on the PG19 test set. Table 3 shows the effect of the token selection

Table 2: MMLU (STEM) evaluation. For results on individual subjects within the STEM category, please see Figures 17 and 18. Higher score is better.

Model	LLaMA2 _{7B} (\uparrow)	Qwen1.5 _{7B} (\uparrow)
Sink Cache	36.02	52.13
Cascade (Ours)	36.20	52.49

method presented in Section 3. We find that without the token selection method, our cache is not effective, and slightly underperforms sink cache. Removing the token selection turns the dynamic attention pattern into a static heuristic, which may drop important context tokens naively.

Table 3: The token selection process outlined in Section 3 is crucial for creating dynamic attention patterns.

KV Cache	Window 2048		Window 4096	
	LLaMA2 _{7B}	Qwen1.5 _{7B}	LLaMA2 _{7B}	Qwen1.5 _{7B}
Sink Cache	7.05	9.70	6.90	9.44
Ours w/o token selection	7.06	9.71	6.91	9.45
Cascade (Ours)	6.97	9.52	6.84	9.33

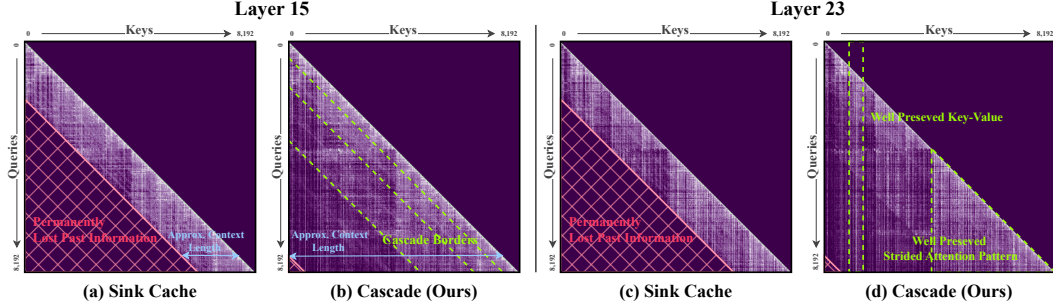


Figure 8: Attention matrix reconstruction for Sink Cache and our Cascading Cache. Both methods result in $\mathcal{O}(n)$ inference time complexity with the same total cache size ($|C| = 2048$).

In Table 5 (bottom), we find that the ideal number of cascades is 4. While the approximate context length increases with a larger number of cascades, it also brings a tradeoff, as the first cascade window will have to be shorter in order to make room for the higher number of sub-caches. For example, with 4 cascades, the first sub-cache which accepts all tokens has a capacity of $|C|/N = 2048/4 = 512$. However, when there are 8 cascades, the first window shrinks to $|C|/N = 2048/8 = 256$. Therefore, there is a shorter window of recent tokens which are collected before beginning to drop tokens. We note that 4 cascades still outperform 1 and 2 cascades, indicating that there is a benefit to lengthening the context window this way, up until the point where the higher overall sparsity becomes a hindrance.

In Table 5 (top left), we show the effect of different frequencies of token acceptance into the sub-caches, where N is the number of sub-cache windows. We find that $\{1/2^{(i-1)}\}_{i=1}^N$ performs best, however, there may be other functions or combinations of functions which may be studied in future works. Table 5 (top right) studies the head reduction function for the token selection process outlined in Section 3. We find that a maximum over the attention heads performs best. Note that all other experiments were performed with mean reduction, which was set as a sensible default.

4.5 Latency

We compare the latency of our cascading cache to the implementation from Xiao et al. [21] which uses tensor concatenation to add/evict keys from the cache. Our implementation utilizes the Triton compiler [18] to create a CUDA kernel for the caching operation. We also do not use a concatenation of tensors to perform the add/evict operations within the cache. We instead instantiate a buffer at initialization, keeping track of the current starting index ξ , and increment it at each addition to the buffer such that $\xi^{(t+1)} = (\xi^{(t)} + 1) \bmod |C_i|$ (i.e. a circular buffer). This way, we know that the oldest token in the buffer resides at the memory address of the starting index. When it is time to remove a token, we simply overwrite the content of the memory address and increment the start index rather than perform a costly concatenation, which requires re-writing all the stored tensor values to a new memory location. To perform this experiment, we initialize a cache with 4 sink tokens and a total window size of $|C| = 1024$ with 4 sub-caches ($N = 4$). We then process a total of 100 tokens as a ‘burn-in’ period to compile and initialize the Triton CUDA kernel. After the burn-in stage, we process a total of 4096 subsequent tokens and report the per-token average latency. Our method with one cascade (equivalent to sink cache) delivers a 59% speedup, and our method with 4 cascades still delivers a 51% speedup over Xiao et al. [21] in addition to the performance gains observed in our experiments.

4.6 Visualization

To visualize the effect of our method, we reconstruct the full attention matrices of sink cache and our method. Note that these are never explicitly constructed in their full form during inference. We used Llama2 7B on the PG19 test set with a total window size of 2048, and 4 cascades for our method. The attention matrices are displayed in Figure 8. Each attention matrix was created using the first 8192 tokens from a single book. As can be seen, naive sliding window attention Figure 8 (a,c) forms a hard barrier where tokens are evicted, forever removing them from the context history and preventing

Table 4: Comparing the latency of a single caching operation between sink cache and our cascading cache.

Method	KV Cache Latency (ms)
Sink Cache [21]	1.33
Sink Cache (Ours w/ 1 cascade)	0.54
Cascade (Ours w/ 4 cascade)	0.64

Table 5: **Top Left:** Frequencies that control the token acceptance rate of each cascade. **Top Right:** Head reduction strategies for the token selection based on attention score Section 3. **Bottom:** Different numbers of cascades will affect the approximate context length. There is a performance tradeoff due to more cascades causing more overall sparsity. All experiments are on PG19 with LLaMA2_{7B}.

Cascade Function	Window 2048			Head Reduction (ρ)	Window 2048		
	$\{1/2^{(i-1)}\}_{i=1}^N$	$\{1/3^{(i-1)}\}_{i=1}^N$	$\{1/4^{(i-1)}\}_{i=1}^N$		Mean	Median	Max
Perplexity	6.97	7.03	7.10	Perplexity	6.97	7.01	6.95

Cascades	Window 2048			
	1	2	4	8
Approx. Context Length	2048	3072	7680	65280
Single Cascade Window Size	2048	1024	512	256
Perplexity	7.05	6.99	6.97	7.18

them from influencing later tokens in the sequence. Our method Figure 8 (b,d) keeps those tokens in the context history for a longer period of time so they may retain influence over future tokens, effectively increasing the available context length in the window.

Under these settings, our approximate context length from Equation (4) is $\frac{2048}{4} \sum_{i=1}^4 2^{i-1} = 7680$. This can be directly observed in Figure 8(b), which shows nonzero attention scores until the bottom left corner. Furthermore, we demonstrate the cascade boundaries of our proposed KV eviction policy in Figure 8(b). It can be seen that the sparsity of each cascade gradually increases with the size of the cascade. Additionally, our method preserves the attention patterns more thoroughly than sink cache, such as the annotated preserved key-value and the strided attention pattern. For un-annotated visualizations from more layers, please see Figures 15 and 16 in the appendix.

5 Limitations & Future Work

Our method operated with the same fixed overhead as sink cache, however, as noted in Equation (4), the size of the first window $|C_1|$ which accepts all incoming tokens will be smaller as the number of cascades N grows larger. This presents a tradeoff, which can also be seen in Table 5 (bottom), as performance increases up until 4 cascades but then decreases as more cascades are added and the level of sparsity rises. The magnitude of this tradeoff is likely dependent on the given task. Promising directions for future work include the study of more sophisticated cascade functions and cache sizing schemes. We employed cascade functions based on simple integer power rules, although there may be other functions or combinations of functions and cache sizes which work well.

Positional embeddings present another possible limitation, as the cache size will be ultimately limited by the number of positional embeddings that the model was pretrained with. Sinusoidal positional embeddings [20, 17] have been shown to degrade performance when extended to longer contexts than were seen during training [15], even though they can theoretically be extended to any length. We note however, that our method efficiently uses the existing positional embeddings by allowing the approximate context length to exceed the number of positional embeddings which are needed, as we only need enough positional embeddings to cover the items in the cache ($|C|$ at most).

6 Conclusion

In this work, we have provided a simple, novel, and effective method for extending the context memory in streaming LLM’s with no training required. Our method views a fixed-sized KV cache as a series of cascading sub-caches, which each accepts tokens with different frequencies. Crucially, we conditionally favor retaining more important tokens (measured by attention score) and evicting less important tokens from the cache, leading to a dynamic context history which a longer approximate context length than a naive sliding window. We provide an efficient implementation which delivers a 59% speedup per caching operation over recent baselines. Compared to sink cache, our method leads to an overall 5.6% improvement on LongBench, a 1.2% improvement on (PG19), and a 0.6% improvement in MMLU(STEM), while retaining linear inference complexity and a fixed memory overhead.

References

- [1] J. Bai, S. Bai, Y. Chu, Z. Cui, K. Dang, X. Deng, Y. Fan, W. Ge, Y. Han, F. Huang, et al. Qwen technical report. *arXiv preprint arXiv:2309.16609*, 2023.
- [2] Y. Bai, X. Lv, J. Zhang, H. Lyu, J. Tang, Z. Huang, Z. Du, X. Liu, A. Zeng, L. Hou, Y. Dong, J. Tang, and J. Li. Longbench: A bilingual, multitask benchmark for long context understanding. *arXiv preprint arXiv:2308.14508*, 2023.
- [3] I. Beltagy, M. E. Peters, and A. Cohan. Longformer: The long-document transformer. *arXiv preprint arXiv:2004.05150*, 2020.
- [4] Y. Chen, S. Qian, H. Tang, X. Lai, Z. Liu, S. Han, and J. Jia. Longlora: Efficient fine-tuning of long-context large language models. *arXiv preprint arXiv:2309.12307*, 2023.
- [5] K. Choromanski, V. Likhoshesterov, D. Dohan, X. Song, A. Gane, T. Sarlos, P. Hawkins, J. Davis, A. Mohiuddin, L. Kaiser, et al. Rethinking attention with performers. *arXiv preprint arXiv:2009.14794*, 2020.
- [6] T. Dao. Flashattention-2: Faster attention with better parallelism and work partitioning. *arXiv preprint arXiv:2307.08691*, 2023.
- [7] I. Han, R. Jayaram, A. Karbasi, V. Mirrokni, D. P. Woodruff, and A. Zandieh. Hyperattention: Long-context attention in near-linear time. *arXiv preprint arXiv:2310.05869*, 2023.
- [8] D. Hendrycks, C. Burns, S. Basart, A. Zou, M. Mazeika, D. Song, and J. Steinhardt. Measuring massive multitask language understanding. *arXiv preprint arXiv:2009.03300*, 2020.
- [9] A. Q. Jiang, A. Sablayrolles, A. Mensch, C. Bamford, D. S. Chaplot, D. d. l. Casas, F. Bressand, G. Lengyel, G. Lample, L. Saulnier, et al. Mistral 7b. *arXiv preprint arXiv:2310.06825*, 2023.
- [10] J.-H. Kim, J. Yeom, S. Yun, and H. O. Song. Compressed context memory for online language model interaction. *arXiv preprint arXiv:2312.03414*, 2023.
- [11] N. Kitaev, Ł. Kaiser, and A. Levskaya. Reformer: The efficient transformer. *arXiv preprint arXiv:2001.04451*, 2020.
- [12] S. Merity, C. Xiong, J. Bradbury, and R. Socher. Pointer sentinel mixture models, 2016.
- [13] A. Mohtashami and M. Jaggi. Landmark attention: Random-access infinite context length for transformers. *arXiv preprint arXiv:2305.16300*, 2023.
- [14] T. Munkhdalai, M. Faruqui, and S. Gopal. Leave no context behind: Efficient infinite context transformers with infini-attention. *arXiv preprint arXiv:2404.07143*, 2024.
- [15] O. Press, N. A. Smith, and M. Lewis. Train short, test long: Attention with linear biases enables input length extrapolation. *arXiv preprint arXiv:2108.12409*, 2021.
- [16] J. W. Rae, A. Potapenko, S. M. Jayakumar, C. Hillier, and T. P. Lillicrap. Compressive transformers for long-range sequence modelling. *arXiv preprint*, 2019. URL <https://arxiv.org/abs/1911.05507>.
- [17] J. Su, M. Ahmed, Y. Lu, S. Pan, W. Bo, and Y. Liu. Roformer: Enhanced transformer with rotary position embedding. *Neurocomputing*, 568:127063, 2024.
- [18] P. Tillet, H.-T. Kung, and D. Cox. Triton: an intermediate language and compiler for tiled neural network computations. In *Proceedings of the 3rd ACM SIGPLAN International Workshop on Machine Learning and Programming Languages*, pages 10–19, 2019.
- [19] H. Touvron, L. Martin, K. Stone, P. Albert, A. Almahairi, Y. Babaei, N. Bashlykov, S. Batra, P. Bhargava, S. Bhosale, et al. Llama 2: Open foundation and fine-tuned chat models. *arXiv preprint arXiv:2307.09288*, 2023.
- [20] A. Vaswani, N. Shazeer, N. Parmar, J. Uszkoreit, L. Jones, A. N. Gomez, Ł. Kaiser, and I. Polosukhin. Attention is all you need. *Advances in neural information processing systems*, 30, 2017.

[21] G. Xiao, Y. Tian, B. Chen, S. Han, and M. Lewis. Efficient streaming language models with attention sinks. *arXiv preprint arXiv:2309.17453*, 2023.

A Appendix

- Appendix B - Derivation of the γ EMA parameter initial setting.
- Appendix C - Detailed explanation of our homogeneous attention head policy for token selection.
- Appendix D - Information regarding the PG19 subset used in our experiments.
- Appendix E - Compute resources used in our experiments.
- Appendix F - Societal Impacts.
- Algorithm 1 - The algorithm of our cascading cache method
- Table 11 - Paths to exact pretrained models used in our experiments.

B EMA Coefficient Derivation

We derived the γ parameter to be dependent on the sub-cache window size such that the influence of attention scores outside the window will decay to $< 1\%$. For example,

$$\boldsymbol{\mu}^{(t+1)} = \gamma \boldsymbol{\mu}^{(t)} + (1 - \gamma) \mathbf{s}_k^{(t)} \quad (5)$$

$$\boldsymbol{\mu}^{(t+1)} = \gamma(\gamma \boldsymbol{\mu}^{(t-1)} + (1 - \gamma) \mathbf{s}_k^{(t-1)}) + (1 - \gamma) \mathbf{s}_k^{(t)} \quad (6)$$

$$\boldsymbol{\mu}^{(t+1)} = \gamma^2 \boldsymbol{\mu}^{(t-1)} + \gamma(1 - \gamma) \mathbf{s}_k^{(t-1)} + (1 - \gamma) \mathbf{s}_k^{(t)} \quad (7)$$

$$\boldsymbol{\mu}^{(t+1)} = \gamma^{t+1} \mathbf{0} + \sum_{i=0}^t \gamma^i (1 - \gamma) \mathbf{s}_k^{(t-i)} \quad (8)$$

$$\boldsymbol{\mu}^{(t+1)} = \sum_{i=0}^t \gamma^i (1 - \gamma) \mathbf{s}_k^{(t-i)} \quad (9)$$

(10)

for the first timestep which is outside of the range of the sub-cache, we set the coefficient such that $\gamma^{\frac{|C|}{N}+1} \leq 0.01$. Therefore,

$$\gamma^{\frac{|C|}{N}} = 0.01 \quad (11)$$

$$\frac{|C|}{N} \ln \gamma = \ln \left(\frac{1}{100} \right) \quad (12)$$

$$\ln \gamma = \frac{-N \ln(100)}{|C|} \quad (13)$$

$$\gamma = \exp \left(\frac{-N \ln(100)}{|C|} \right) \quad (14)$$

We analytically set this hyperparameter as a sensible default. For the cache sizes used in our experiments, this formula results in the following values for γ ,

Table 6: Settings for the EMA γ coefficient for our experiments based on the size of the cascading sub-caches $\frac{|C|}{N}$ as described in Equation (11).

$\frac{ C }{N}$	$\frac{2048}{4}$	$\frac{4096}{4}$
γ	0.991	0.995

We performed an ablation study in the setting of γ and found that our method is insensitive to the setting.

Table 8: Tabular display of radar plot results from Figure 7. Our cascade models all use 4 sub-caches ($N = 4$) in this experiment. Higher scores are better (\uparrow)

Window	Model	Cache	Narrative QA	HotPot QA	Qasper	Multi News	2 Wiki MQA	Gov. Report	Mean
1024	LLaMA2 _{7B}	Sink Cache	6.21	8.95	6.31	23.93	9.21	22.28	12.81
		Cascade (Ours)	6.5	9.93	7.66	23.29	9.6	23.22	13.36
1024	Qwen1.5 _{7B}	Sink Cache	12.22	25.75	23.15	22.66	23.92	22.45	21.69
		Cascade (Ours)	15.44	30.11	28.94	22.5	25.89	24.43	24.55
2048	LLaMA2 _{7B}	Sink Cache	6.69	8.95	9.15	24.41	9.98	24.55	13.95
		Cascade (Ours)	6.54	10.95	8.23	24.78	10.27	24.7	14.24
2048	Qwen1.5 _{7B}	Sink Cache	13.19	29.36	29.58	23.48	28.32	24.42	24.72
		Cascade (Ours)	17.99	33.37	30.91	22.92	28.73	26.25	26.69
1024	LLaMA2 _{13B}	Sink Cache	8.83	10.25	9.35	21.38	13.89	20.58	14.04
		Cascade (Ours)	8.31	9.52	11.21	23.57	14.42	21.17	14.70
1024	Qwen1.5 _{14B}	Sink Cache	15.83	35.99	22.6	22.09	28.97	24.55	25.00
		Cascade (Ours)	17.59	36.18	30.06	22.37	27.89	25.23	26.55
2048	LLaMA2 _{13B}	Sink Cache	9.15	9.77	12.1	24.76	13.7	21.66	15.19
		Cascade (Ours)	7.99	11.71	8.9	24.75	14.16	23.6	15.18
2048	Qwen1.5 _{14B}	Sink Cache	18.46	39.42	30.39	23.26	32.82	25.14	28.24
		Cascade (Ours)	19.69	41.89	30.85	22.57	34.05	26.13	29.19

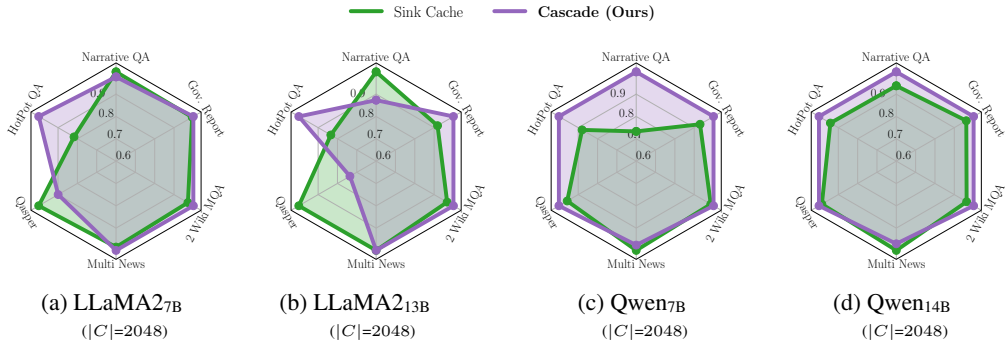


Figure 9: LongBench [2] results in addition to those presented in Figure 7.

Table 7: PG19 perplexity results for LLaMA2_{7B} ($N = 4$, $|\mathcal{C}| = 2048$) when changing the EMA hyperparameter γ . We find our model to be insensitive to the setting of γ .

Setting	$\exp\left(\frac{-N \ln(10)}{ \mathcal{C} }\right)$	$\exp\left(\frac{-N \ln(100)}{ \mathcal{C} }\right)$	$\exp\left(\frac{-N \ln(1000)}{ \mathcal{C} }\right)$
γ value	0.995	0.991	0.986
Perplexity	6.975	6.971	6.970

C On Homogeneous Attention Head Retention/Eviction Policy

Table 9: Perplexity on the PG19 test subset. An independent heal policy causes the cache to make a heterogeneous action during the token selection process, causing a misalignment of positional encodings.

Window	Model	Homogeneous Head Policy	Independent Head Policy (Naive)
2048	LLaMA2 _{7B}	6.97	10.95

As mentioned in Section 3, we perform a reduction across the attention heads of every token before updating the attention score EMA. This causes our cache to take the same token selection action across all heads of every token. While it is possible to allow the token selection to happen independently across the heads, it poses a problem for the positional embeddings because we must then apply different positional embeddings across the attention heads if the heads came from a different original token. This could potentially cause a large increase in the number of positional

encodings required, and could exceed the available positional embeddings in a given model (example depicted in Figure 10). We attempted naively applying positional encodings from an independent head policy by applying a single positional encoding index where heads from different tokens would have been mixed together by an independent head policy (Figure 10 right), but the performance degradation was severe (Table 9). Therefore, we opted to use a homogeneous head policy, which we found to work well and efficiently utilize the available positional encodings.

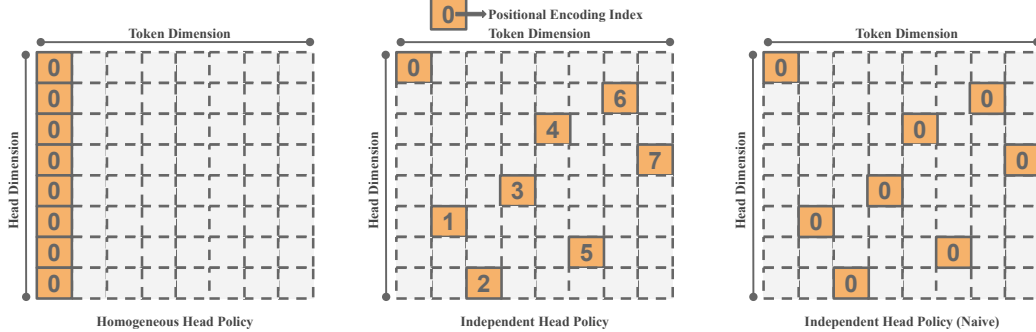


Figure 10: Using an independent head policy would allow for the token selection to choose individual heads from different token indices. This increases the number of positional encodings required, as heads may be mixed from tokens with different initial positions.

D PG19 Test Subset

For our experiments on PG19, we chose a subset of the test set consisting of 25 full-length books. We chose the books by sorting the test by total length in tokens, and then selecting a sequential set of 25 books starting with those that are near the maximum limit (32k) of the pretrained models we use.

Table 10: List of book indices and token lengths for the PG19 subset we used for our experiments. Token lengths are based on the tokenizer for Llama2.

book index	11	41	7	94	66	39	40	70	25	59	46	47	20
length (tokens)	31673	32515	32948	39062	39332	41026	41435	42381	42773	43094	43169	45040	46529
book index	22	85	51	77	86	24	62	34	36	95	5	0	-
length (tokens)	46531	48183	51459	52302	54233	55270	57485	59273	63470	63518	64672	65134	-

E Compute Requirements

We utilize three nodes consisting of NVIDIA 8X 2080Ti, 8X A100, and 8X A6000 GPU’s for our experiments. We report the latency of our method/implementation in Table 4. We utilize half precision (16-bit) for all experiments. The largest model we use consists of 14 Billion parameters, which consumes approximately 28GB of GPU memory which may be distributed among multiple GPU’s using tensor parallelism.

F Societal Impacts

We are not aware of any possible negative societal impacts of our work that are above and beyond any that may exist for general LLM’s. We do however, note a possible positive impact of our work which works towards closing the gap between quadratic and linear attention during inference. Upon deployment, this would greatly decrease decoding latency, energy costs, and required compute resources for any organization who runs an LLM in production.

Algorithm 1 Cascading Sink Cache Algorithm (repeat for keys and values)

Require: cascade_cache_buf_array, sink_cache_buf, score_cache, item_to_cache

```
if not sink_cache_buffer.is_full() then
    sink_cache_buffer ∪ item_to_cache
    return
end if
for cache_buf in cascade_cache_buf_array do
    if cache_buf.is_accepting_tokens() then
        if not cache_buf.is_full() then
            cache_buf ∪ item_to_cache
            update_positional_encoding()
            return
        else
            cache_buf ∪ item_to_cache
            item_to_cache ← cache_buf.evict_oldest()           ▷ reset variable for next iteration
            update_positional_encoding()
        end if
    else
        if cache_buf.is_empty() then
            cache_buf ∪ item_to_cache
            update_positional_encoding()
            return
        else
            newest_item ← cache_buf.get_newest_item()          ▷ eager add to empty cache to avoid naively evicting
            newest_score ← score_cache.get(newest_item)
            item_score ← score_cache.get(item_to_cache)
            if item_score > newest_score then
                cache_buf.evict_newest()
                cache_buf ∪ item_to_cache
                update_positional_encoding()
            end if
            return
        end if
    end if
end if
end for
```

Model	Huggingface Path	Experiment
LLaMA2 _{7B} 32k [19]	togethercomputer/LLaMA-2-7B-32K	PG19,MMLU,Ablation
LLaMA2 _{13B} 32k [19, 4]	Yukang/Llama-2-13b-longlora-32k-ft	PG19
LLaMA2 _{7B} Chat 32k [19]	togethercomputer/Llama-2-7B-32K-Instruct	LongBench
LLaMA2 _{13B} Chat 32k [19]	Yukang/Llama-2-13b-chat-longlora-32k-sft	LongBench
Qwen1.5 _{7B} [1]	Qwen/Qwen1.5-7B	PG19,MMLU,Ablation
Qwen1.5 _{7B} Chat [1]	Qwen/Qwen1.5-7B	LongBench
Qwen1.5 _{14B} [1]	Qwen/Qwen1.5-14B	PG19
Qwen1.5 _{14B} Chat [1]	Qwen/Qwen1.5-14B	LongBench

Table 11: Huggingface model paths used in our experiments.

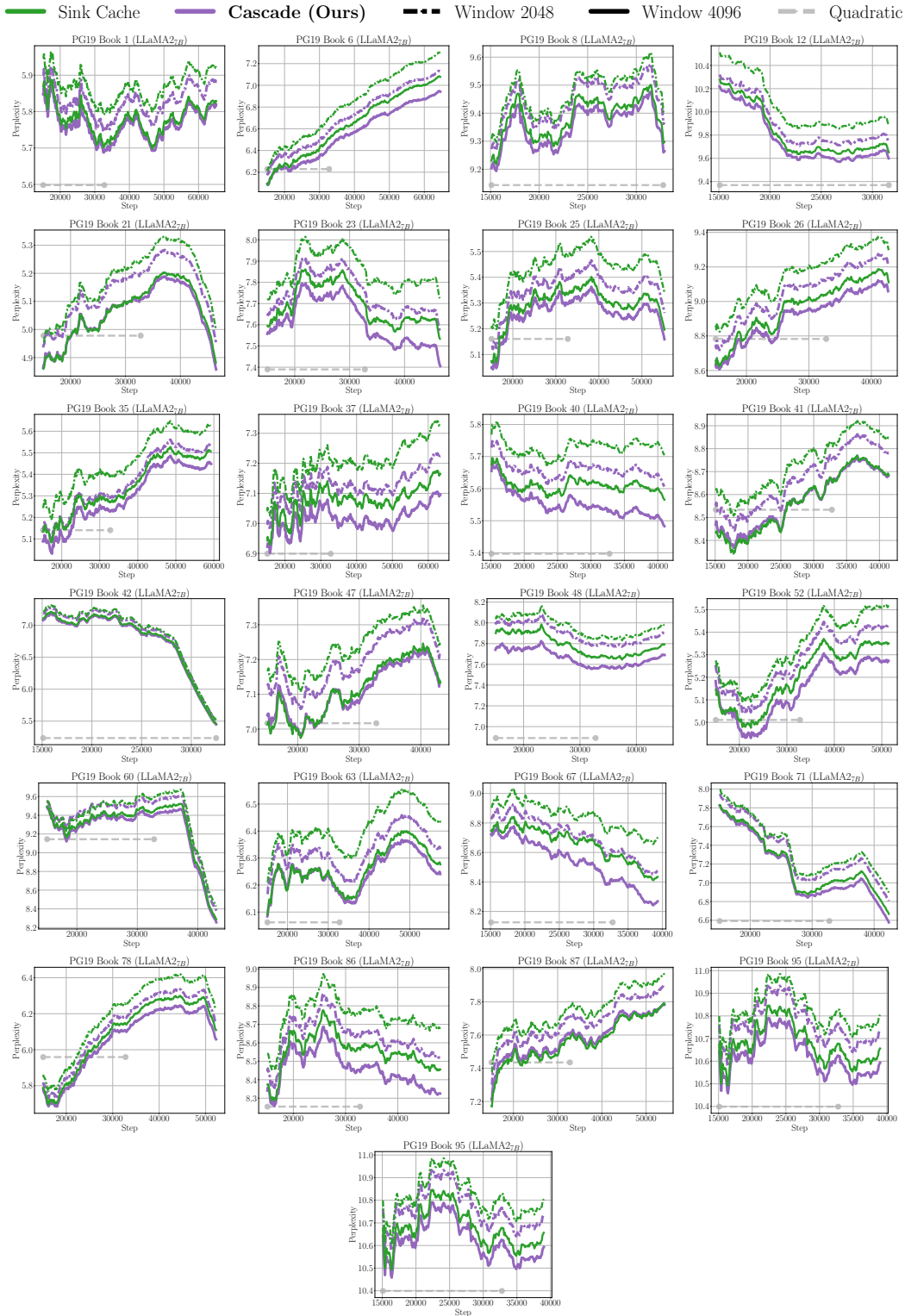


Figure 11: LLaMA2_{7B} per book average perplexity measurements during the entire stream of a single book. The plotted line represents the average perplexity at the given step (i.e. $\exp\left(\frac{1}{N} \sum_{i=1}^N \text{CE}(x_i, y_i)\right)$)

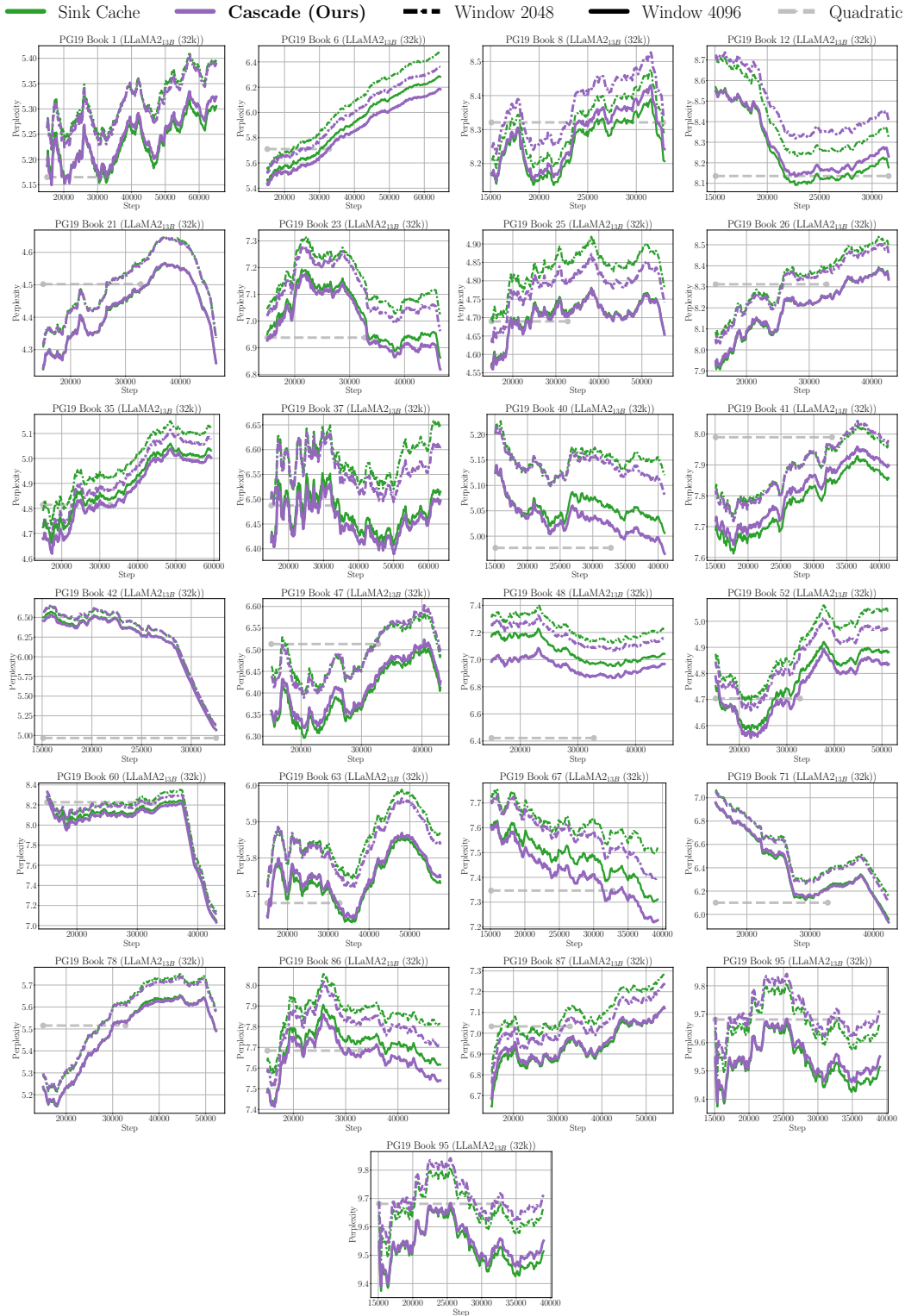


Figure 12: LLaMA2_{13B} per book average perplexity measurements during the entire stream of a single book. The plotted line represents the average perplexity at the given step (i.e. $\exp\left(\frac{1}{N} \sum_{i=1}^N \text{CE}(x_i, y_i)\right)$)

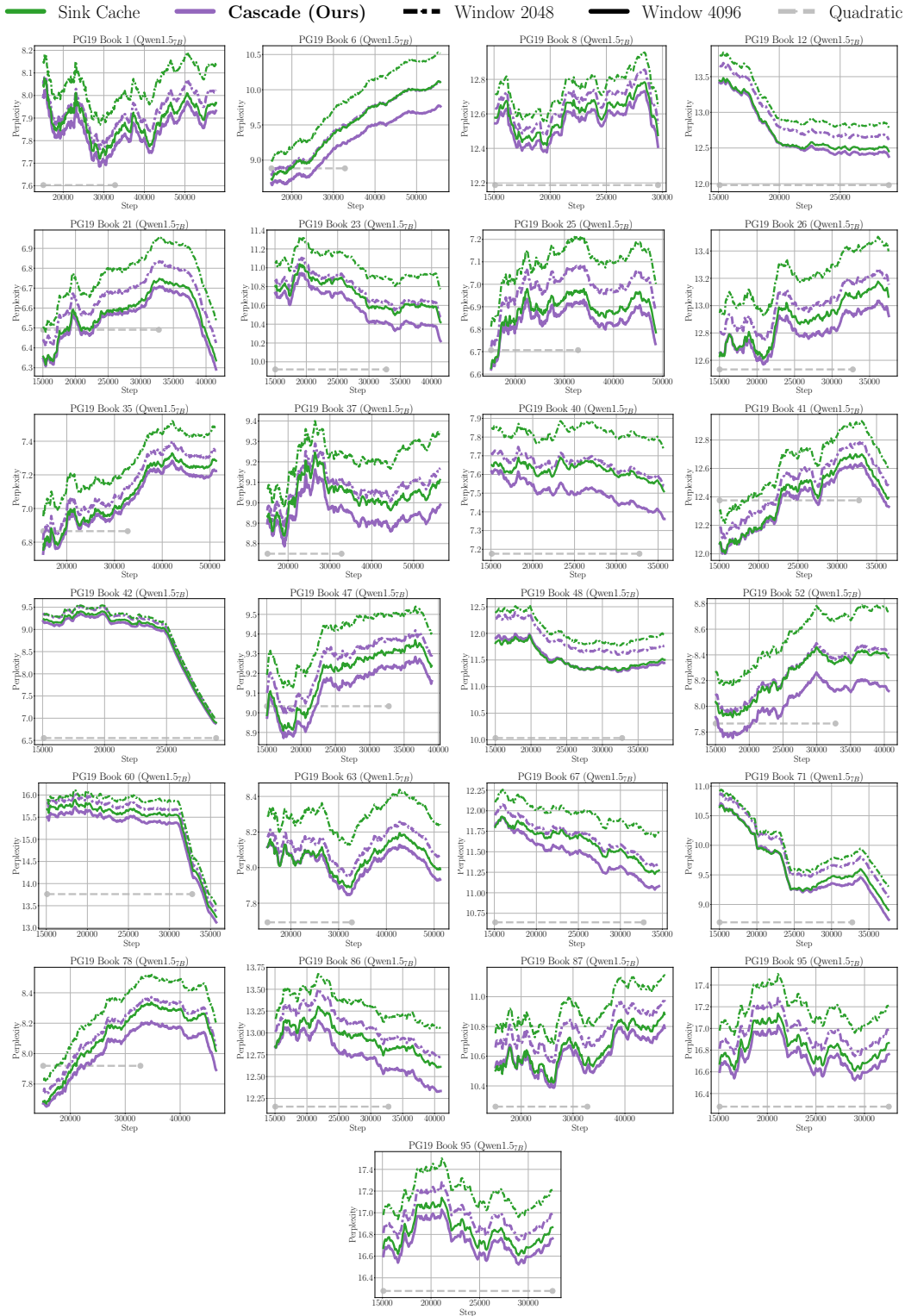


Figure 13: Qwen1.5_{7B} per book average perplexity measurements during the entire stream of a single book. The plotted like represents the average perplexity at the given step (i.e. $\exp\left(\frac{1}{N} \sum_{i=1}^N \text{CE}(x_i, y_i)\right)$)

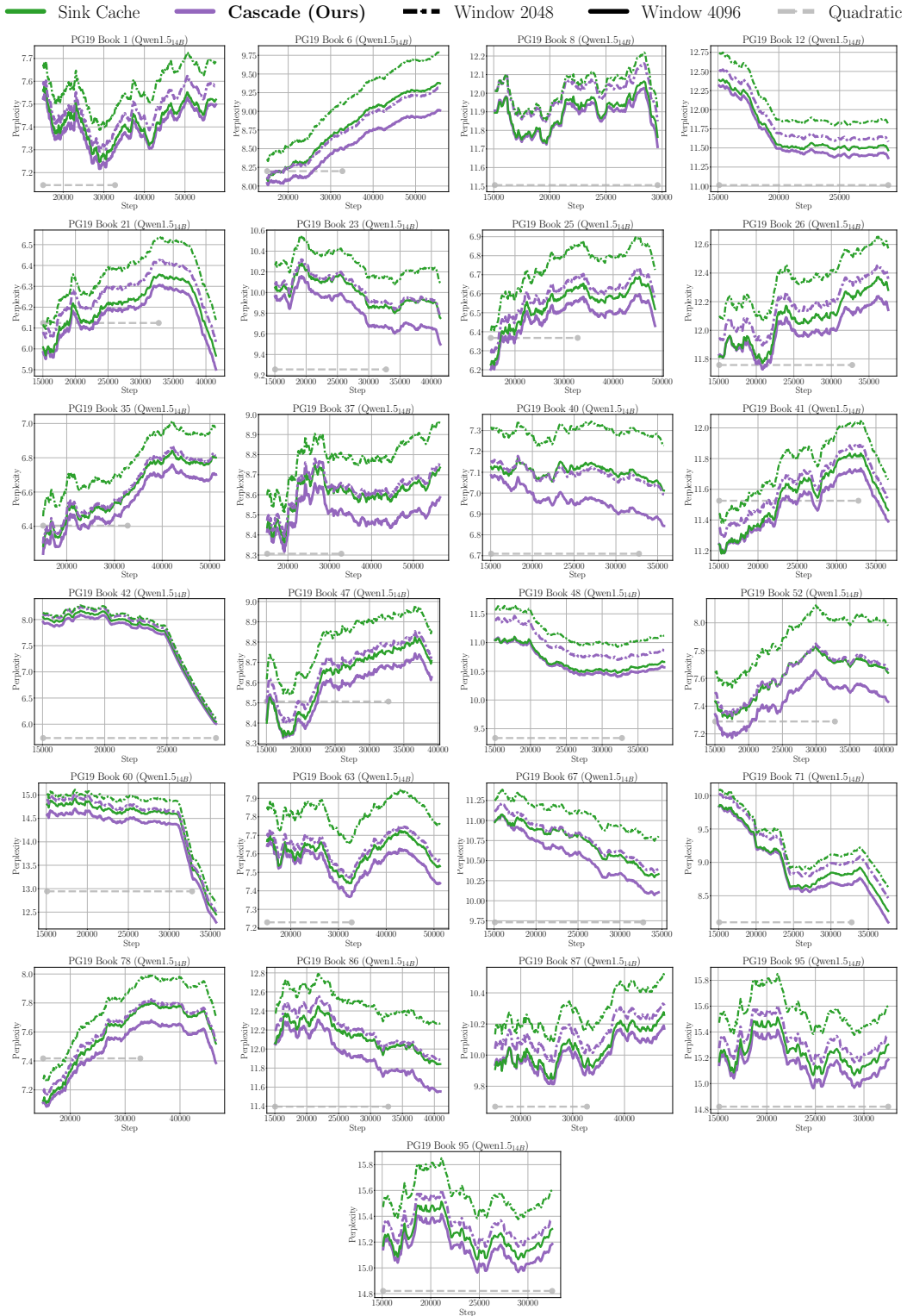


Figure 14: Qwen1.5_{14B} per book average perplexity measurements during the entire stream of a single book. The plotted line represents the average perplexity at the given step (i.e. $\exp\left(\frac{1}{N} \sum_{i=1}^N \text{CE}(x_i, y_i)\right)$)

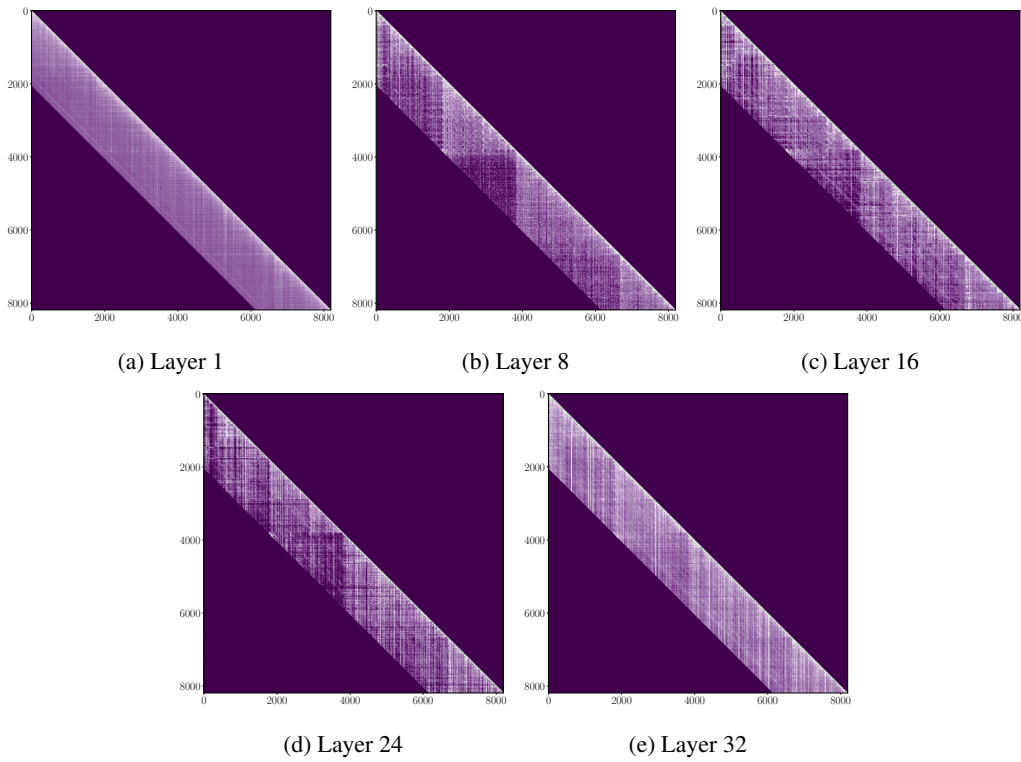


Figure 15: Attention matrix reconstructions for Sink Cache (PG19).

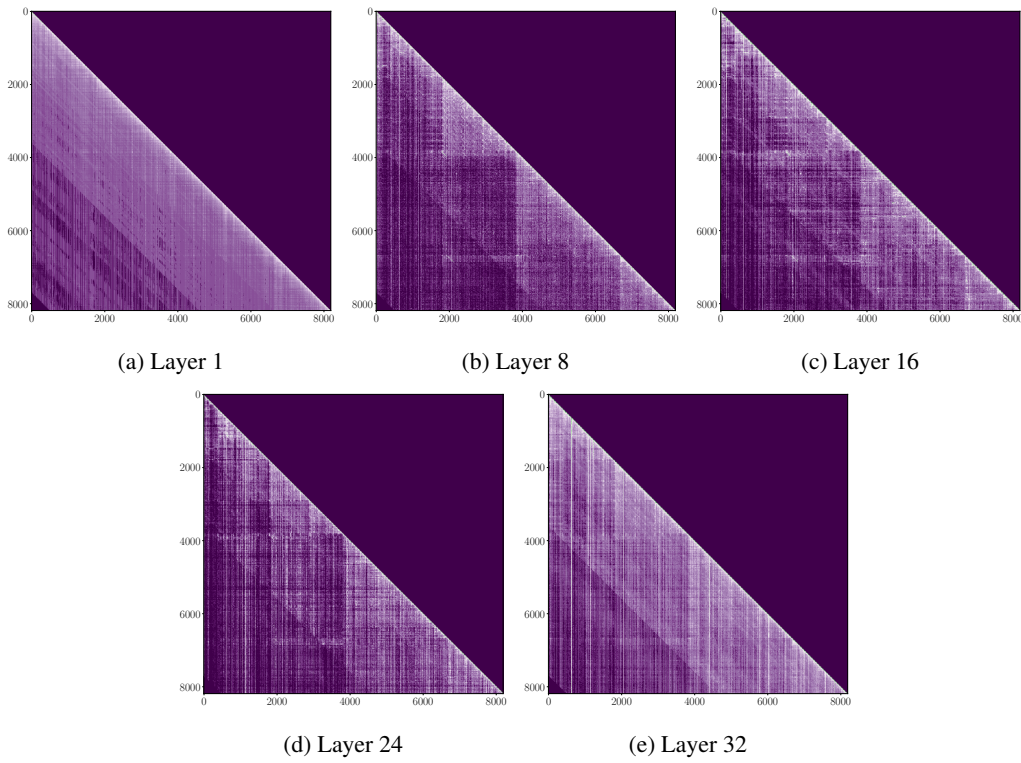


Figure 16: Attention matrix reconstructions for our Cascading KV Cache (PG19).

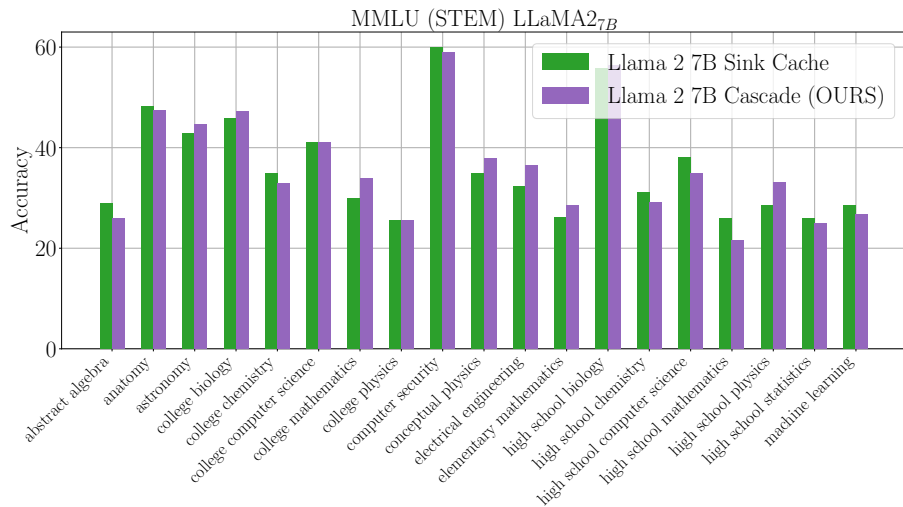


Figure 17: MMLU results for LLaMA2_{7B}

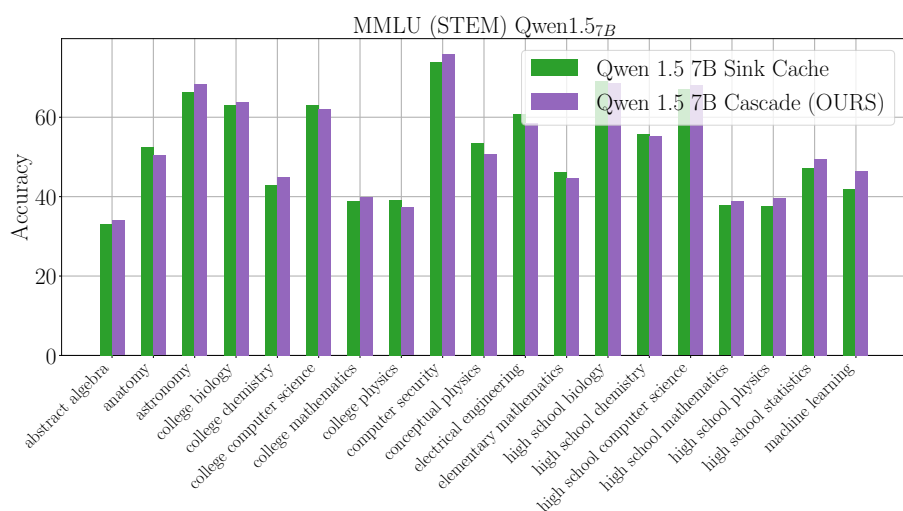


Figure 18: MMLU results for Qwen1.5_{7B}